JET-P(95)69

Collective Thomson Scattering using a Gyrotron from JET Plasmas

J A Hoekzema, H Bindslev, J Egedal,
J A Fessey, T P Hughes[1].

JET Joint Undertaking, Abingdon, Oxfordshire, OX14 3EA, UK.
[1] Dept. of Physics, University of Essex, Colchester, Essex, CO4 3SQ, UK.

Preprint of an Invited Paper to be submitted for publication in
the proceedings of the 7th LAPD

November 1995

7th International Symposium on Laser-Aided Plasma Diagnostics
Fukuoka, Japan, 5-8 December 1995

Collective Thomson Scattering Using a Gyrotron from JET Plasmas

J.A. Hoekzema, H. Bindslev, J. Egedal, J.A. Fessey, T.P. Hughes*
JET Joint Undertaking, Abingdon, Oxfordshire, OX14 3EA, UK.
* and Dept. of Physics, University of Essex, Colchester, Essex, CO4 3SQ, UK

Abstract

A collective Thomson scattering diagnostic has recently come into operation at JET. The diagnostic uses a 500 kW, 140 GHz gyrotron as the source of probing radiation and will be used to measure the spatially resolved velocity distribution of fast alpha particle populations when JET enters the DT phase. First measurements were aimed at the measurement of the thermal ion feature. The diagnostic behaved as expected and the observed signal to noise ratios were satisfactory, indicating that the diagnostic should give the expected performance for observation of fast ion and alpha particle populations in the next operational phase of JET.

Introduction

At a frequency of 140 GHz, the spectrum of scattered radiation is dominated by collective scattering up to scattering angles of at least 60° for JET plasma parameters. Provided the scattering vector is not chosen close to perpendicular to the magnetic field direction, the ion velocity distribution along the scattering vector can be determined from the spectrum [1]. The thermal ions form a narrow central feature in the scattered spectrum. Measurement of this feature was the object of the initial diagnostic operation reported here. The main aim of the diagnostic will be the measurement of the velocity distribution of fast ions, especially alpha particles created by fusion reactions when JET enters the DT phase. Alpha particles, slowing down in the plasma from a birth energy of 3.5 MeV, form a distinctive feature which extends to larger frequency shifts. The spectral region where this feature dominates the spectrum contains information on the alpha particle velocity distribution above ~0.5 MeV. The diagnostic system at JET has steerable launch and receive beams, and different directions of the scattering vector and different spatial regions in the plasma can be selected. The possibility to measure at different scattering vector directions is important when the velocity distribution is non-isotropic, as is the case for fast ion populations generated by the heating systems.

The frequency of 140 GHz was chosen because it is the only frequency where relatively large scattering angles can be used, the plasma is accessible for the normal range of densities (at least for magnetic fields above 3 T) and a source with sufficiently high power and long pulse length was (eventually) available. The injected power has to be modulated to discriminate between the scattered radiation and the much brighter (by 2 orders of magnitude) background radiation (ECE). Fluctuations on the background radiation are the main source of noise for the measurement. It is expected that, when JET will produce DT plasmas with parameters near scientific breakeven, the alpha particle feature can be measured with typical s/n ratio ~10 (for the detection channel bandwidth of $\Delta v/5$) when integration times ~ 100 ms are used.

Diagnostic system

A schematic overview of the diagnostic is given in fig 1. Only a brief description is given here with emphasis on the initial performance. A more detailed description of the system can be found elsewhere [2-4].

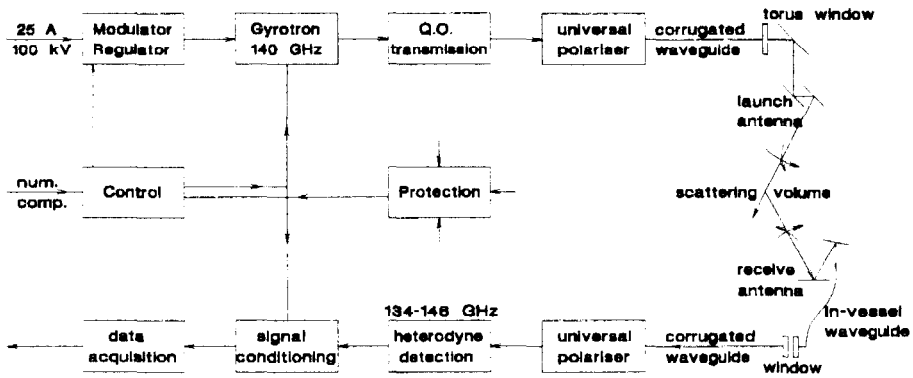

Figure 1: *Schematic overview of the diagnostic*

The gyrotron is operated at 70 kV/ 25 A beam voltage/current and can generate 500 kW RF at 140 GHz for 0.5 s. It is important that the RF output is spectrally clean (i.e. power in spurious frequencies in the spectral range of interest > 80 dB down on power in the main frequency) because radiation in spurious frequencies, entering the receiver as stray light, cannot be discriminated from scattered radiation. Spurious frequencies were observed during switch-on and switch-off but not during the flat top of the pulse except at the highest power levels. For this reason the gyrotron was operated at slightly reduced voltage and ~90% of maximum power. It is likely that the power can be slightly raised when the stability of the 70 kV supply voltage is further improved. The present gyrotron is operated at lower voltage/higher current than the gyrotron originally envisaged for this diagnostic and during initial operation the pulse length was limited by the power supply to ~ 20 ms. The gyrotron is a diode-type tube and modulation of the output power is possible by modulating the beam voltage: Fast modulation of the beam voltage was not yet available for the initial operation (the gyrotron originally envisaged had a modulating anode) and instead the gyrotron was switched on at 120 Hz for a number of pulses of 1 ms duration.

The output of the gyrotron is mainly (>90%) in a Gaussian beam. The high power transmission line (fig 2) uses a combination of quasi-optical and waveguide propagation. The first part of the transmission system is quasi-optical. Most of the non-Gaussian power is lost from the beam in this section. The leakage power is effectively contained within the enclosure around the gyrotron and quasi-optical transmission line, as was verified by measurements. This section includes a polariser to produce the desired elliptical polarisation to couple to either the Ordinary or the eXtraordinary mode in the plasma. The power in 2 orthogonal polarisations is monitored.

The Gaussian beam is then coupled into oversized (ID 88.9 mm) corrugated waveguide in which the radiation propagates in the $HE_{1,1}$ mode. Proper alignment of the beam into the waveguide and of the waveguide itself is crucial to avoid significant mode conversion, which would affect the quality of the beam at the end of the waveguide. When the alignment was imperfect, arcing occurred shortly after the end of the waveguide.

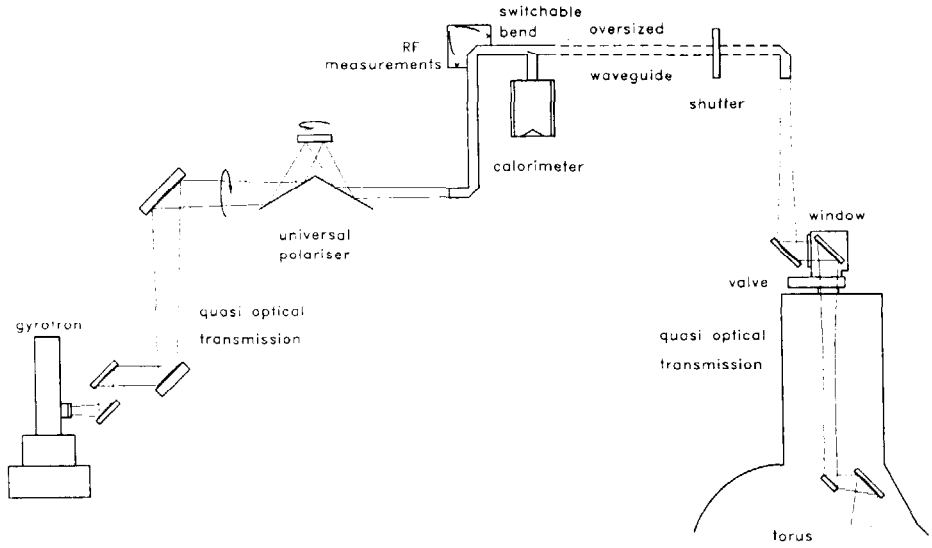

Figure 2: *The high power 140 GHz transmission system*

With correct alignment, the transmission efficiency of the 60 m long waveguide run, which includes 7 mitre bends, was extremely good and no loss of power was measured by comparing the pulse time necessary to blacken thermo-sensitive paper at the beginning and the end of the waveguide. Also, the burn pattern at the end of the waveguide was closely Gaussian (figure 3).

Figure 3: *Burn pattern on thermosensitive paper of the beam radiated from the end of the waveguide. The granular structure is due to reflection on a gramular absorber placed below the paper.*

The last part of the high power transmission line is again quasi optical and a focused Gaussian beam, with waist radius 30 mm at the plasma centre, is launched into the torus via a steerable mirror from a top port. The torus vacuum window was a single disk fused silica window with resonant thickness to avoid reflection. The heating rate of a waterfree fused silica window was measured at 100 °C/s during full power transmission, indicating there should be no problem transmitting the full pulse length through this type of window. An increase of the reflection during transmission due to the change of optical properties when the window is heated, will be avoided when the window is replaced with a double disk window (required for the DT phase) with optimum distance between the disks. The RF power level at the torus was about 370 kW. For the antenna orientations used in the first measurements, only about 10 mW was coupled to the receiver as stray light. Surprisingly, when firing into an empty torus, the power coupled to other microwave diagnostics was at least an order of magnitude below the damage level of the most sensitive detectors, indicating that the effective reflectivity of the JET vessel wall is quite low (<70%). No precautions are therefore necessary to avoid firing into the torus when no plasma (which is an effective dump for the microwaves after reflection) is present.

The receive beam also has a waist of 60 mm in the plasma centre and the spatial resolution for the measurement is therefore around 100 mm, dependent on the chosen scattering angle. Via a steerable mirror, the receive beam is focused into corrugated waveguide, which initially has a

small diameter (ID 10 mm) to allow curvature around the divertor systems in the bottom of the torus. It is tapered up to 31.75 mm in the bottom port and is continued for ~40 m to the detection system where the radiation is coupled into fundamental waveguide via a polariser. The attenuation in the main receive waveguide run is only a few dB. Absolute calibration of the full receiver transmission line will be done before the next operational phase using a calibrated noise source in the vessel. For the initial experiments, relative calibration was obtained by assuming the radiation from the plasma (ECE) is constant in the spectral range of interest and approximate absolute calibration by comparing these signals with those measured by a calibrated ECE diagnostic (although this has a different viewing line through the plasma). Calibration of the antenna directions was based on a measurement of the mirror angles inside the vessel during the previous shutdown. The estimated uncertainty is ~ 1° (this will also be further improved before the next campaign). Apart from the main receiver, there are 4 slave receivers with viewing directions around the main receiver viewing direction, to check beam overlap. These slave receivers were not connected during the initial measurements. Instead, optimum overlap was established by scanning the main receiver beam between shots. Before the detection system, 2 fundamental waveguide notch filters in series removed the stray light. The stray light attenuation at the centre frequency was at least 80 dB and the full notch width 200 MHz at -3 dB. The heterodyne detection system measures the spectrum between 134 and 146 GHz in 32 channels. The channel bandwidth is chosen to be proportional to the frequency shift. For the measurement of the thermal ion feature only ~10 channels closest to the central frequency are of interest. Of these, calibration of the most central 2 or 3 channels is somewhat uncertain due to the effect of the notch filters. The data acquisition system includes a real time signal averager but it was not necessary to use this for the first short pulse measurements.

Results

For the initial measurement the O-mode was selected both for injection and detection. The X-mode can be used at densities up to ~ 5.10^{19} m^{-3} and gives higher scattering signals but the signal level is not a problem for measurement of the thermal ion feature and refraction effects are more important for the X-mode. Ray tracing calculations were done to calculate the required antenna directions and polariser settings for an expected plasma. The scattering volume was placed in the centre of the plasma and a scattering vector $|\mathbf{k}|$ = 1500 m^{-1} was chosen. The scattering angle was 32° and the angle between **k** and **B**, 122°. In operation, only the viewing direction of the receiver beam was adjusted to optimise the overlap. The scattering parameters are slightly different for different plasma parameters, due to the effect of refraction, and were recalculated using the actual plasma parameters. In practice, optimum overlap of the launch and receive beams was lost whenever the plasma magnetic configuration or the density was significantly changed. Generally, a number of similar plasmas were required to optimise the overlap. It should be easier to find the optimum overlap when the slave receivers are operational.

Clear scattering signals were seen from plasmas with $B_0 > 3$ T [5]. A sample of the raw data is given in figure 4. These data were taken shortly after a sawtooth collapse. It is seen that the background radiation is going down (cooling of the outer region where this radiation is emitted) while the scattering signal goes up (re-heating of the central region where the scattering volume is located). For this particular discharge, the scattered radiation in the centremost channels was higher than expected, indicating there may still be an effect of non-thermal density fluctuations up to a frequency shift of 100 MHz.

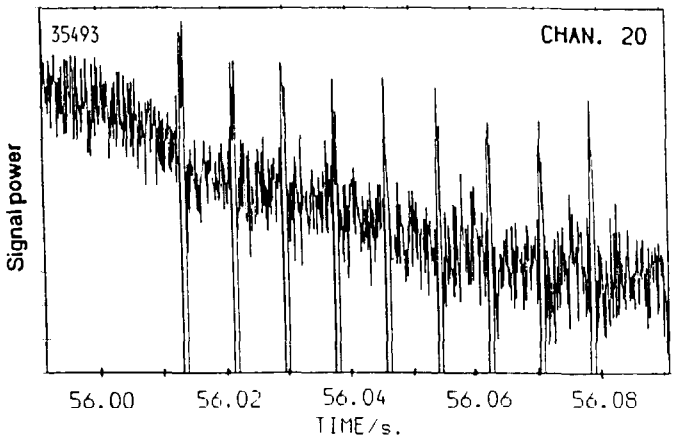

Figure 4: *Raw data at $\Delta v \approx 600$ MHz from a plasma with $B = 3.1$ T, $n_e = 3.10^{19}$ m^{-3}, T_e $T_i = 3$ keV, 1.4 MW hydrogen minority heating (ICRH). Nine 1 ms pulses are injected at 120 Hz.*

It is also clearly seen from fig. 4 that during switch-on and switch-off of the gyrotron the receiver is saturated. This is due to spurious frequencies generated during switch-on and switch-off which are outside the notch and enter the receiver as stray light. In some channels, at frequencies where spurious signals are present, positive spikes are seen during these periods. Although the receiver seems to recover quickly from these spikes, detailed analysis shows that there are still some saturation effects during the gyrotron pulse. It is possible that this is due to a relatively high power level at frequencies where the detection system is blind, i.e. at frequency shifts around 50 MHz where the notch filters start to transmit. For fast ion measurements, when much smaller scattering signals have to be detected, it will be important to avoid these effects (by using a wider notch filter and proper modulation).

At magnetic field values below 3 T no clear scattering signals were found. This was expected since 2nd harmonic absorption starts to interfere around 3 T. At $B \approx 2.9$ T, signals were observed in some channels but these channels are not centred around the injected frequency. An example is given in fig. 5.

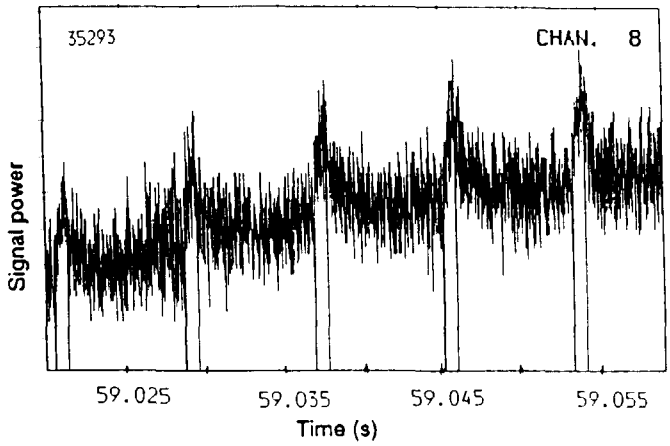

Figure 5: *Raw data from a plasma with $B = 2.9$ T showing a "heating signal".*

The signal shows a linear rise during the pulse and a gradual decay after the pulse which clearly identifies it as a heating signal: The power is absorbed in the outer plasma layer, which increases the electron temperature locally and enhances the ECE background radiation at frequencies where the receiver observes this layer. To some extent this effect must also be present at other magnetic fields (although not noticeble with the short integration times used during these measurements), because the injected radiation is absorbed in the plasma after reflection off the wall. This is the main reason why fast (10 kHz) modulation will be necessary for fast ion and alpha particle measurements. In the absence of plasma, no signals were observed except during switching and in the channel at the gyrotron frequency.

An example of a scattering spectrum is given in fig. 6. The histogram represents the measured spectral intensity in each channel normalised to that of ECE at 140 GHz, which in this case was at a rather high level of 900 eV (for comparison, the alpha feature will only have a radiation temperature of a few eV). A theoretical fit is also given, based on B, n_e and T_e values from other diagnostics while the ion parameters are fitted. The fit is only illustrative. It assumes that the central peaks are due to Nitrogen. The shift of ~ 30 MHz could be induced by a toroidal drift velocity of 1.6. 10^5 m/s. Power accountability is quite good (although the absolute calibration is only approximate): The absolute level of the measured spectral intensity is ~ 80% of that predicted by theory for perfect beam overlap. The post detection signal to noise ratio, defined as the ratio of the scattered signal to the fluctuations on the total signal, varies over the spectrum between ~ 10 and ~100. Similar values are found for other spectra.

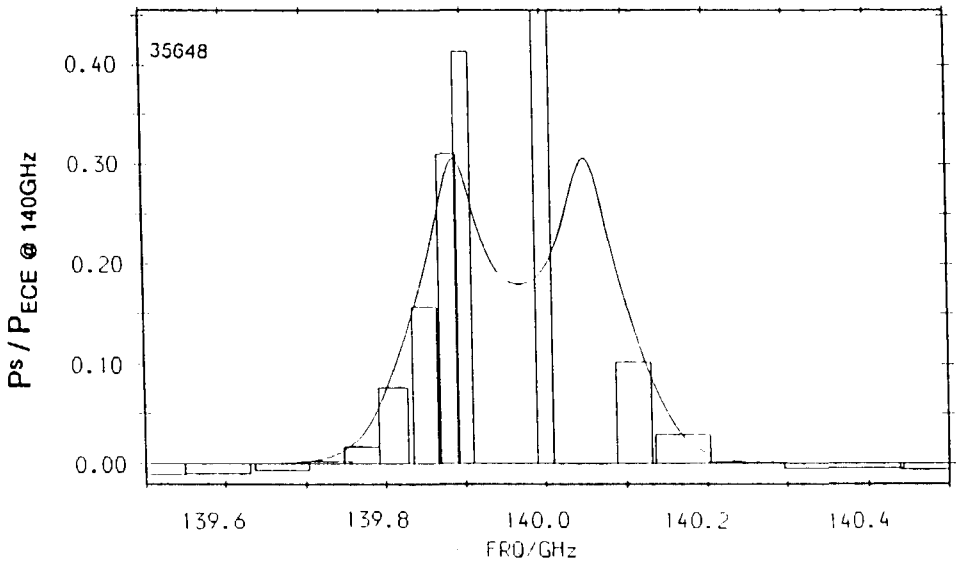

Figure 6. *Example of a measured spectrum of scattered radiation from a plasma with 6 MW ICRH, 10 MW NBI, B=3.1 T, n_e 4.7.10^{19} m^{-3}, T_e 3.2 keV. The curve gives the theoretically fitted spectrum using n_D 2.7.10^{19} m^{-3}, T_D 2.5 keV, n_N 0.28.10^{19} m^{-3}, T_N 2.5 keV.*

Conclusion

The initial operation of the diagnostic was useful to test the system, to demonstrate its viability and to identify areas where further improvements can be made. The results confirmed expectations and signal to noise ratios were in satisfactory agreement with theory.

References

[1] H. Bindslev, this conference and references therein
[2] A.E. Costley et.al. JET Report R(88)08(1988)
[3] J.A. Hoekzema et.al., Proc. 2nd Int. Workshop on Strong Microwaves in Plasmas, Volga, Russia (1993)
[4] J.A. Hoekzema et.al., Proc. 17th Int. Conf. on IR and mm Waves, Colchester, UK, (1992), pp 579, 588 and 244
[5]. J.A. Hoekzema et.al., 22nd EPS Conf. on Contr. Fusion and Plasma Phys., Bournemouth (1995), II -445